行政院國家科學委員會補助專題研究計畫成果報告

※※※※※※※※※※※※※※※※※※※※※※※※※
※ ※
※ **仿生型自主式水下載具運動性能之研究(I)** ※
※ ※
※※※※※※※※※※※※※※※※※※※※※※※※※

計畫類別：□個別型計畫 à整合型計畫
計畫編號：NSC89－2611－E－002－018
執行期間：88 年 8 月 31 日至 89 年 7 月 31 日

計畫主持人：邱逢琛

本成果報告包括以下應繳交之附件：
□赴國外出差或研習心得報告一份
□赴大陸地區出差或研習心得報告一份
□出席國際學術會議心得報告及發表之論文各一份
□國際合作研究計畫國外研究報告書一份

執行單位：國立台灣大學造船及海洋工程學系

中　華　民　國　89 年 10 月 31 日

行政院國家科學委員會專題研究計畫成果報告

仿生型自主式水下載具運動性能之研究(I)

Study on the Motions of Biomimetic AUVs (I)

計畫編號: NSC89-2611-E-002-018
執行期限:88 年 8 月 1 日至 89 年 7 月 31 日

主持人: 邱逢琛　台灣大學造船及海洋工程學系
計畫參與人員：郭振華　台灣大學造船及海洋工程學系
吳兆平　台灣大學造船及海洋工程學系

I. Abstract

The main purpose of this research is to simulate the undulatory locomotion of a flexible body. When a flexible slender body which is divided into a number of segments undulates, the wave passes from the nose to the tail. Reaction forces due to momentum change, friction, as well as cross flow drag acting on each segment are taken into account. Equations of motion described by the body-fixed coordinate are obtained by taking the summation of the longitudinal force, lateral force and yaw moment acting on all the segments. Equations of motion are solved step by step in time axis and the velocity is transferred to space-fixed coordinate. The trajectory of the flexible body can be obtained by time integration of the transferred velocity. Results are obtained for the numerical model in which length, outline dimensions of each segment are similar to a test vehicle we are currently building. The validity and limitation of the simulation method are discussed.

Keywords: Undulatory locomotion, Flexible slender body, Biomimetic AUV

中文摘要

無人水下載具在複雜的海底進行檢測作業時，經常需要如底棲魚類那樣能低速徘徊、準確到位、敏捷迴旋的能力，尤其在浮遊狀態下操作機械手臂時，更是需要極為精緻的運動操控能力。我們知道為了使載具停止並保持浮游姿勢，必須反覆且迅速產生正反推力，而這正是利用傳統螺槳推進方式最為困難之處。相對於此，魚類胸鰭的往復運動（Oscillatory Motion）以及包含魚體和尾鰭在內的波動運動（Undulatory Motion）則顯然能較輕易且優雅的使魚類做到。 因此，從模仿魚類運動著手，以期探究出提升自主式水下載具低速徘徊運動操控性能、高速巡航推進效率的新方法, 並思索出具協調能力之 AUV 群體的基本架構，就是本群體研究計畫的動機。而其具體目標則是經由對魚類外型、感知、行為、運動機制的模擬，建構出仿生型自主式水下載具試驗機 (BAUV testbed)。為達上述目標，本群體研究整合了五個子計畫, 分別進行仿生型 AUV 的阻力推進性能（子計畫一）、運動性能（子計畫二）、行為控制系統（子計畫三）、視覺感測及知覺系統（子計畫四）、幾何外型設計與決策規劃（子計畫五）等相關之基礎研究。

魚類外形因生活形態之需，經長期演化而成的最適化外形，通常是下述三種運動性能的妥協，即巡航與衝刺(Cruising & Sprinting)、突進(Accelerating)、操控(Maneuvering)等三種運動性能。而前二者主要關係到包含魚體和尾鰭在內的波動運動（Undulatory Motion），後者則主要關係到魚類胸鰭的往復運動（Oscillatory Motion），然而通常還更可能包括魚體、尾鰭、胸鰭的同時運動與交互影響，譬如行進中的急速迴旋運動。是故，為求建立針對仿魚 BAUV 以運動性能為基礎的最佳化外形設計(Motion-based design)之能力，本子計畫（子計畫二）擬以三年為期致力於魚類運動機制的探究，如停留、轉向、突進、急煞等運動機制之解明與再現模擬，並進行實驗驗證。而其第一年之主要研究目的在於建立包含魚體與尾鰭在內之

魚類波動運動之數學模式，並蒐集運動相關之流體動力係數，以進行魚類運動模擬計算。

本成果報告將敘述細長撓性體波動推進之運動模擬，內容包括其理論推導、數值計算方法，並以本整合型計畫建構中的仿生自主式水下載具之外型為例進行模擬計算之探討。

關鍵詞: **波動推進、撓性細長體、仿生自主式水下載具**

II. INTRODUCTION

There is currently an increased interest in the use of Autonomous Underwater Vehicles (AUVs) for oceanographic, military and commercial missions. Existing AUVs are small robotic submarines powered by rotary propellers driven by electric motors. The low efficiency of the small diameter propellers coupled with the large fraction of the hull volume required to hold the motor's batteries leads to short mission times, restricted payloads and control problems. To emulate the ability of easy and elegant hovering, accurate positioning and agile turning motion of fishes, the propulsion system of the AUV must generate positive and inverse thrust quickly and repeatedly. This can keep the AUV still in the water and maintain its buoyant position, which is difficult for traditional propeller propulsion systems to achieve.

To explore the possibility of possible gains by mimicking the design of comparably sized biological systems, we are planning to build a fish-like underwater vehicle as a testbed to investigate interactions and coordination among appearance, motion, behavior, and perception. In order to develop such a so-called Biomimetic Autonomous Underwater Vehicle (BAUV) which is propelled by the undulatory motion of a flexible hull or the swing of paired fins, it should be helpful in the preliminary design stage to have a practical tool to simulate the locomotion by the undulatory motion of a flexible body.

For 'elongated' fishes which are geometrically characterized by slender cylindrical forms, Lighthill developed the elongated-body reactive-force theory [1]. Lighthill investigated the inviscid flow around a slender fish which makes swimming movements in a direction transverse to its direction of locomotion, while its cross-section varies along it only gradually. Based on the slender-body theory, Lighthill obtained the result of thrust produced by the fish, time-rate of work done by it, and the rate of shedding of energy, showing that the mean values of these quantities all depend on the movement and body shape at the tail-end section only, and that they will vanish with the virtual mass of the tail. What has primarily been implied here is that the body cross-section varies so gradually, and its shape is so smooth (no sharp edges), that the cross-flow remains attached to body, leaving no vortex sheet until the tail-end section is reached [2].

Wu made further investigations on this problem [3]. In order to simplify the mathematical analysis, Wu limited the consideration to the ribbon-fin-type problem, assuming that the trailing side-edges have a gradual change in slope, but are sharp enough to shed an oscillating vortex sheet from the body in an undulatory swimming motion. There are other discussions about propulsion by median and paired fins by Blake [4][5], the geometric mechanics of undulatory robotic locomotion [6][7] and analysis of swimming propulsion of a three-dimensional waving plate with variable amplitudes [8].

In this paper, a practical simulation method developed under slender body assumption will be presented. The length of the flexible slender body is divided into a number of segments. When the body undulates, the wave passes from the nose to the tail. Due to momentum change, friction and cross flow drag, the reaction forces are taken into account by each segment. The equations of motions described by the body-fixed coordinate are obtained by taking the summation of the longitudinal force, lateral force and yaw moment acting on all the segments, respectively. The equations of motions are solved step by step in time axis using the Newmark- direct method at each

time step. The velocity described by the body-fixed coordinate are then transferred to the space-fixed coordinate and we can obtain the trajectory by time integration of the transferred velocity.

Fortran language is used for the program design. Behavior of a BAUV testbed currently being built will be studied.

III. MATHEMATICAL MODELING

We have three coordinate systems (Figure 1): space-fixed coordinate system $O-XY$, body-fixed coordinate system $o-xy$ (global) and segment-fixed coordinate system $\tilde{o}_i-\tilde{x}_i\tilde{y}_i$ (local). Each coordinate can be transferred to another coordinate by using the relationship of the position and angle between two coordinate systems.

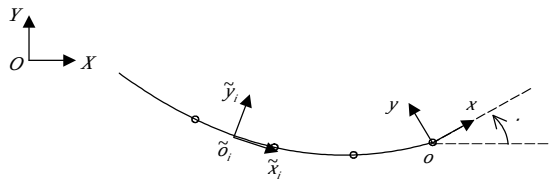

Figure 1 Definitons of coordinae systems

From observations of biological fishes [10][11], the motion can be considered as traveling waves that increase in amplitude from the nose to the tail. A specific form of traveling wave equation which is a slight derivation from that originally suggested by Lighthill [2] was developed. Let the body-spline take the form of a traveling wave given by:

$$y(x,t) = (c_1 x + c_2 x^2)\sin(kx+\mu t)\cdot(1-e^{-\frac{t}{T}}) \qquad (1)$$

where:

y = transverse displacement of body

x = displacement along main axis

$k = \frac{2\pi}{\lambda}$ = body wave number

λ = body wave length

c_1 = coefficient of linear wave amplitude envelope

c_2 = coefficient of quadratic wave amplitude envelope

$\mu = 2\pi f = \frac{2\pi}{T_{body}}$ = body wave frequency

T = period of the initial undulating delay cycle

This is the equation of a sinusoidal wave traveling from right to left (i.e. from $x=0$ to $x=-L$) within the bounds of a second-order ($c_1 x + c_2 x^2$) amplitude envelope [12]. The exponential term is to simulate the initial delay when the body starts to undulate. The slope of the body is,

$$y_x(x,t) = \frac{\partial y}{\partial x}$$
$$= \left[(c_1 x + c_2 x^2)k\cos(kx+\mu t) + (c_1 + 2c_2 x)\sin(kx+\mu t)\right]\cdot(1-e^{-\frac{t}{T}}) \qquad (2)$$

the angle between the body and the x-axis is $\theta \equiv \tan^{-1} y_x$

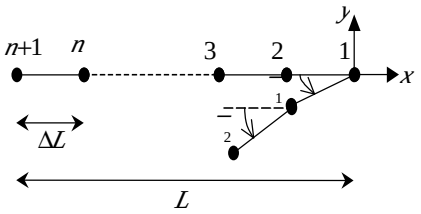

Figure 2 Representation of body segments

Dividing the whole body into n segments (Figure 2), then the length of each segment is $\Delta L = L/n$, and the coordinates of two nodes of the i^{th} segment are (x_i, y_i), (x_{i+1}, y_{i+1}).

We have

$$\begin{cases} x_1 = y_1 = 0 \quad , \quad \theta_1 = \tan^{-1} y_x(\frac{\Delta L}{2}, t) \\ x_i = x_{i-1} - \Delta L\cos\theta_{i-1} \quad , \quad 2 \le i \le n+1 \\ y_i = y_{i-1} - \Delta L\sin\theta_{i-1} \quad , \quad 2 \le i \le n+1 \\ \theta_i = \tan^{-1} y_x(x_i - \frac{\Delta L}{2}\cos\theta_{i-1}, t) \quad , \quad 2 \le i \le n \end{cases} \qquad (3)$$

Next, we will derive motion equations in the body-fixed coordinate system, $o-xy$.

(i) The horizontal moving velocity vector described by body-fixed coordinate system is $(u(t), v(t), 0)$, angular velocity vector is $(0, 0, \omega(t))$. Assuming that the center of the i^{th} segment $(\bar{x}_i, \bar{y}_i)$ is the center of mass of that segment which has mass of m_i, and $\bar{x}_i = \frac{x_{i+1}+x_i}{2}$, $\bar{y}_i = \frac{y_{i+1}+y_i}{2}$. The rotating inertial torque is I_i (with center of mass as the rotating center). Thus, the horizontal velocity of $(\bar{x}_i, \bar{y}_i)$ caused by ω is:

$$\begin{vmatrix} \vec{i} & \vec{j} & \vec{k} \\ 0 & 0 & \dot{\theta} \\ \bar{x}_i & \bar{y}_i & 0 \end{vmatrix} = (-\bar{y}_i \dot{\theta})\vec{i} + (\bar{x}_i \dot{\theta})\vec{j}$$

and the horizontal velocity of $(\bar{x}_i, \bar{y}_i)$ caused by undulation in x direction ≈ 0, in y direction is $y_t(\bar{x}_i, t) = \dfrac{\partial y(\bar{x}_i, t)}{\partial t}$.

For fluid added mass effect, use the total differential of $y(\bar{x}_i, t)$:

$$\frac{dy}{dt} = \dot{y} = y_t - u y_x$$

$$\frac{d^2 y}{dt^2} = \ddot{y} = y_{tt} - u y_{xt} - \dot{u} y_x - u(y_{tx} - u y_{xx})$$

Thus, we can get the horizontal velocity and acceleration in y direction for added mass as: (where $\bar{v}_i^*$ and $\dot{\bar{v}}_i^*$ are for body mass)

$$\bar{v}_i = v + \bar{x}_i \dot{\theta} + y_t - u y_x \equiv \bar{v}_i^* - u y_x$$

$$\dot{\bar{v}}_i = \dot{v} + \bar{x}_i \ddot{\theta} + y_{tt} - u y_{xt} - \dot{u} y_x - u(y_{tx} - u y_{xx})$$

$$= \dot{v} + \bar{x}_i \ddot{\theta} + y_{tt} - \dot{u} y_x - 2u y_{xt} + u^2 y_{xx} \equiv \dot{\bar{v}}_i^* - \dot{u} y_x - 2u y_{xt} + u^2 y_{xx}$$

Horizontal velocities and angular velocities described in the body-fixed coordinate system $o - xy$ are:

$$\begin{cases} \bar{u}_i(t) = u(t) - \bar{y}_i \dot{\theta} \\ \bar{v}_i(t) = v(t) + \bar{x}_i \dot{\theta} + y_t(\bar{x}_i, t) - u y_x(\bar{x}_i, t) \\ \bar{v}_i^*(t) = v(t) + \bar{x}_i \dot{\theta} + y_t(\bar{x}_i, t) \\ \dot{\theta}_i(t) = \dot{\theta} + \dfrac{\partial(\tan^{-1} y_x(\bar{x}_i, t))}{\partial t} = \dot{\theta} + \dot{\theta}_i \end{cases} \tag{4}$$

and horizontal accelerations and angular accelerations are:

$$\begin{cases} \dot{\bar{u}}_i(t) = \dot{u}(t) - \bar{y}_i \ddot{\theta} - \dot{u} y_t(\bar{x}_i, t) + u \dot{y}_x(\bar{x}_i, t) \\ \dot{\bar{u}}_i^*(t) = \dot{u}(t) - \bar{y}_i \ddot{\theta} - \dot{u} y_t(\bar{x}_i, t) \\ \dot{\bar{v}}_i(t) = \dot{v}(t) + \bar{x}_i \ddot{\theta} + y_{tt}(\bar{x}_i, t) - \dot{u} y_x(\bar{x}_i, t) - 2u y_{xt}(\bar{x}_i, t) + u^2 y_{xx}(\bar{x}_i, t) \\ \dot{\bar{v}}_i^*(t) = \dot{v}(t) + \bar{x}_i \ddot{\theta} + y_{tt}(\bar{x}_i, t) \\ \ddot{\theta}_i(t) = \ddot{\theta} + \dfrac{\partial^2(\tan^{-1} y_x(\bar{x}_i, t))}{\partial t^2} = \ddot{\theta} + \ddot{\theta}_i \end{cases} \tag{5}$$

In the segment-fixed coordinate system $\tilde{o}_i - \tilde{x}_i \tilde{y}_i$, the horizontal velocity and the angular velocity of the i^{th} segment for fluid added mass effect are:

$$\begin{cases} \tilde{u}_i = \bar{u}_i \cos\theta_i + \bar{v}_i \sin\theta_i \\ \tilde{v}_i = \bar{v}_i \cos\theta_i - \bar{u}_i \sin\theta_i \\ \dot{\theta} = \dot{\theta}_i = \dot{\theta} + \dot{\theta}_i \end{cases} \quad \ldots\ldots \tag{6}$$

the horizontal acceleration and angular acceleration are:

$$\begin{cases} \dot{\tilde{u}}_i = \dot{\bar{u}}_i \cos\theta_i + \dot{\bar{v}}_i \sin\theta_i \\ \dot{\tilde{v}}_i = \dot{\bar{v}}_i \cos\theta_i - \dot{\bar{u}}_i \sin\theta_i \\ \ddot{\theta} = \ddot{\theta}_i = \ddot{\theta} + \ddot{\theta}_i \end{cases} \tag{7}$$

For body masses, horizontal velocities and accelerations are:

$$\begin{cases} \tilde{u}_i^* \equiv \bar{u}_i \cos\theta_i + \bar{v}_i^* \sin\theta_i \\ \tilde{v}_i^* \equiv \bar{v}_i^* \cos\theta_i - \bar{u}_i \sin\theta_i \end{cases} \tag{8}$$

$$\begin{cases} \dot{\tilde{u}}_i^* \equiv \dot{\bar{u}}_i \cos\theta_i + \dot{\bar{v}}_i^* \sin\theta_i \\ \dot{\tilde{v}}_i^* \equiv \dot{\bar{v}}_i^* \cos\theta_i - \dot{\bar{u}}_i \sin\theta_i \end{cases} \tag{9}$$

The representations of horizontal angular velocity and acceleration for body masses are the same as shown in (7).

Consider each segment as a rigid body, the Euler-Lamb equation of the i^{th} segment described in the segment-fixed coordinate system $\tilde{o}_i - \tilde{x}_i \tilde{y}_i$ is:

$$\begin{cases} m_i \dot{\tilde{u}}_i^* - m_i \tilde{v}_i^* \dot{\theta}_i + m_{x_i} \dot{\tilde{u}}_i - m_{y_i} \tilde{v}_i \dot{\theta}_i = F_{vxi} \\ m_i \dot{\tilde{v}}_i^* + m_i \tilde{u}_i^* \dot{\theta}_i + m_{y_i} \dot{\tilde{v}}_i + m_{x_i} \tilde{u}_i \dot{\theta}_i = F_{vy_i} \\ (I_{zi} + J_{zi}) \ddot{\theta}_i + (m_{y_i} - m_{xi}) \tilde{u}_i \tilde{v}_i = G_{vzi} \end{cases} \tag{10}$$

The fluid viscous forces at the right side of the above equation are composed of friction C_f (in the $\tilde{x}$ direction), and cross flow drag C_d (in the $\tilde{y}$ direction).

$$F_{vxi} = -\tfrac{1}{2} \rho \tilde{u}_i^2 \cdot C_f \cdot S_i$$

$$F_{vxi} = -\tfrac{1}{2} \rho \tilde{v}_i^2 \cdot C_d \cdot d_i \cdot \Delta L$$

where

S_i: the wet surface area of the i^{th} segment

d_i: the height of the cross-section of the i^{th} segment (perpendicular to the y-axis), and

$$G_{vzi} = -2 \cdot \int_0^{\frac{\Delta L}{2}} \tfrac{1}{2} \rho (l\dot{\theta})^2 \cdot l \cdot C_d \cdot d_i \cdot dl$$

$$= -\rho \dot{\theta}^2 C_d d_i \int_0^{\frac{\Delta L}{2}} l^3 \, dl$$

$$= -\rho \dot{\theta}^2 C_d \cdot d_i \cdot \frac{(\Delta L)^4}{64}$$

In summary, we can know that forces acting on the i^{th} segment described in the $\tilde{o}_i - \tilde{x}_i \tilde{y}_i$ system are:

$$\begin{cases} F_{\tilde{x}_i} = -m_i \dot{\tilde{u}}_i^* + m_i \tilde{v}_i^* \dot{r} - m_{x_i} \dot{\tilde{u}}_i + m_{y_i} \tilde{v}_i \dot{r} - \frac{1}{2} \rho \tilde{u}_i^2 \cdot C_f \cdot S_i \\ F_{\tilde{y}_i} = -m_i \dot{\tilde{v}}_i^* - m_i \tilde{u}_i^* \dot{r} - m_{y_i} \dot{\tilde{v}}_i - m_{x_i} \tilde{u}_i \dot{r} - \frac{1}{2} \rho \tilde{v}_i^2 \cdot C_d \cdot d_i \cdot \Delta L \\ G_{\tilde{z}_i} = -(I_{z_i} + J_{z_i}) \ddot{r} - (m_{y_i} - m_{x_i}) \tilde{u}_i \tilde{v}_i - \rho \dot{r}^2 C_d \cdot d_i \cdot \frac{(\Delta L)^4}{64} \end{cases} \quad (11)$$

(iii) The forces acting on the i^{th} segment described in the body-fixed coordinate system $o-xy$ are:

$$\begin{cases} F_{x_i} = F_{\tilde{x}_i} \cos \psi_i - F_{\tilde{y}_i} \sin \psi_i \\ F_{y_i} = F_{\tilde{x}_i} \sin \psi_i + F_{\tilde{y}_i} \cos \psi_i \\ G_{z_i} = G_{\tilde{z}_i} \end{cases} \quad (12)$$

(iv) The forces and torques acting on the whole body described in the body-fixed coordinate system $o-xy$ are:

$$\begin{cases} \sum_{i=1}^{n} F_{x_i} = 0 \\ \sum_{i=1}^{n} F_{y_i} = 0 \\ \sum_{i=1}^{n} G_{z_i} + \sum_{i=1}^{n} (F_{y_i} \bar{x}_i - F_{x_i} \bar{y}_i) = 0 \end{cases} \quad (13)$$

(v) Finally, we can get the motion equations in the $o-xy$ system as:

$$\begin{cases} A_{11}\dot{u} + A_{12}\dot{v} + A_{13}\dot{r} + B_{11}u + B_{12}v + B_{13}\psi = E_1 \\ A_{21}\dot{u} + A_{22}\dot{v} + A_{23}\dot{r} + B_{21}u + B_{22}v + B_{23}\psi = E_2 \\ A_{31}\dot{u} + A_{32}\dot{v} + A_{33}\dot{r} + B_{31}u + B_{32}v + B_{33}\psi = E_3 \end{cases} \quad (14)$$

or,

$$[A]\begin{Bmatrix} \dot{u} \\ \dot{v} \\ \dot{r} \end{Bmatrix} + [B]\begin{Bmatrix} u \\ v \\ \psi \end{Bmatrix} = \begin{Bmatrix} E \end{Bmatrix} \quad (15)$$

where $[A]$, $[B]$, $\{E\}$ are known values. One can use a standard numerical integration method, such as the Newmark- method, to obtain $(\dot{u}, \dot{v}, \dot{r})$ and (u, v, ψ).

IV. Numerical Simulation

4.1 Program Description

From the derivation of the Newmark- integration method:

$$\psi = \psi_0 + \Delta t \cdot \dot{\psi}_0 + \frac{1}{2}\Delta t^2 \ddot{\psi}_0 + \beta \Delta t^2 (\ddot{\psi} - \ddot{\psi}_0) \quad (16)$$

The horizontal velocity in the $o-xy$ system described in the $O-XY$ system is:

$$\begin{cases} U = u \cos \psi - v \sin \psi \\ V = u \sin \psi + v \cos \psi \end{cases} \quad (17)$$

The trajectory of the $o-xy$ in the $O-XY$ system are:

$$\begin{cases} X(t) = X_0 + \Delta t \cdot U_0 + \frac{1}{2}\Delta t^2 \dot{U}_0 + \beta \Delta t^2 (\dot{U} - \dot{U}_0) \\ Y(t) = Y_0 + \Delta t \cdot V_0 + \frac{1}{2}\Delta t^2 \dot{V}_0 + \beta \Delta t^2 (\dot{V} - \dot{V}_0) \end{cases} \quad (18)$$

and the trajectory of the nodes of each segment are:

$$\begin{cases} X_i(t) = X(t) + (x_i \cos \psi - y_i \sin \psi) \\ Y_i(t) = Y(t) + (x_i \sin \psi + y_i \cos \psi) \end{cases} \quad (19)$$

The simulation procedure is described as follows:

(i) Input the main characters of the model simulated

Dimensions (total length, the width and height of the cross-section of each segment), friction and cross flow drag coefficients, C_f and C_d. The parameters of wave equation: c_1, c_2, k, μ and T.

(ii) Calculate m_i, m_{xi}, m_{y_i}, S_i, d, I_{zi} and J_z of each segment. Elliptical function was used to represent the shape of the cross-section.

$$m_i = \rho a_i b_i \cdot \Delta L$$
$$m_{x_i} \approx 0$$
$$m_{y_i} = \rho b_i^2 \cdot \Delta L$$
$$S_i \approx circumference\ of\ ellipse \times \Delta L$$
$$d_i = 2b_i$$
$$I_{zi} = Fac \times m_i$$
$$J_{zi} = Fac \times m_{y_i}$$

where $Fac = \frac{1}{4}r^2 + \frac{1}{12}\Delta L^2$, $r = \frac{a+b}{2}$

(iii) Decide how many cycles will be calculated in the program, and how many time steps in one cycle.

(iv) Start the calculation

At t=0, the initial velocity and acceleration is 0. At each time step, the values of the velocity and acceleration of the previous time step will be used to calculate the velocity and acceleration described by body-fixed coordinate of the current time step. The trajectory of the body are then obtained by transferring the velocity and acceleration to the space-fixed coordinate.

Artificial springs are applied to avoid drifting in the y direction and over-rotating of the angle ψ. The reason of using artificial springs is that there are no input force terms in the motion of sway and yawing. Any accumulated error on numerical calculation in the motion of sway and yawing may affect

the result of calculation because each time step involved with the previous time step, and it may cause the drifting in the y direction and over-rotating of the angle $\cdot$. Therefore, two artificial springs are added into the motion equations of sway and yawing.

$$Fac_{sway} = spring\ ratio_{sway} \cdot (\frac{\mu}{2})^2 \cdot m$$

$$Fac_{yaw} = spring\ ratio_{yaw} \cdot (\frac{\mu}{2})^2 \cdot I$$

where $m = \sum m_i$, $I = \sum m_i \bar{x}_i^2$

Thus, the motion equation of (15) becomes:

$$[A]\begin{Bmatrix} \dot{u} \\ \dot{v} \\ \dot{r} \end{Bmatrix} + [B]\begin{Bmatrix} u \\ v \\ r \end{Bmatrix} = \begin{Bmatrix} E_1 \\ E_2 \\ E_3 \end{Bmatrix} - \begin{Bmatrix} Fac_{sway} Y \sin \cdot \\ Fac_{sway} Y \cos \cdot \\ Fac_{yaw} \cdot \end{Bmatrix} \qquad (20)$$

and with the application of the Newmark-method, equation (20) becomes:

$$\left\{[A] + \frac{\Delta t}{2}[B]\right\}\begin{Bmatrix} \dot{u} \\ \dot{v} \\ \dot{r} \end{Bmatrix} = \begin{Bmatrix} E_1 \\ E_2 \\ E_3 \end{Bmatrix} - \begin{Bmatrix} Fac_{sway} Y \sin \cdot \\ Fac_{sway} Y \cos \cdot \\ Fac_{yaw} \cdot \end{Bmatrix} - \frac{\Delta t}{2}[B]\begin{Bmatrix} \dot{u}_0 \\ \dot{v}_0 \\ \dot{r}_0 \end{Bmatrix} - [B]\begin{Bmatrix} u_0 \\ v_0 \\ r_0 \end{Bmatrix} \qquad (21)$$

The values of the previous time step are used for Y and $\cdot$ in the right side of the equation (21) as their initial values, then proceed the iteration with corrected values in each cycle until the acceleration that satisfies the matrix equation is obtained. Then spring forces acting on the motion of sway and yawing take effect when the body drifts or over-rotates.

4.2 Simulation Case

This is a case in which length, outline dimensions of each segment are similar to the BAUV testbed we are currently building.

(i) Model description

total length: $L = 1.6$ (m)

the body is divided into 18 sections, $\Delta L = \frac{1.6}{18} = 0.089$ (m)

the width and the height of the cross-section of each segment, a and b are shown in Table 1.

(ii) Friction and cross flow drag coefficients

C_f (from ITTC 1957)

$$C_F = \frac{0.075}{(\log(\mathrm{Re}) - 2)^2} = \frac{R_f}{\frac{1}{2} \cdot U^2 S} = 4.24 \times 10^{-3}$$

(for $20^o c$ water, $\nu \approx 1.0 \times 10^{-6}\ m^2/\mathrm{sec}$. If assume that $U \approx 1\ m/\mathrm{sec}$, then $\mathrm{Re} = \frac{UL}{\nu} \approx 1.6 \times 10^6$ for $L = 1.6$ m)

C_d (from Handbook of Fluid Dynamics, Fig. 13.9 and Table 13.3)

$$\begin{cases} body\ (taken\ as\ a\ cylinder) & C_D = \dfrac{D}{\frac{1}{2} \cdot U^2 h} = 1.2 \\ tail\ (taken\ as\ a\ flat\ plate) & C_D = \dfrac{D}{\frac{1}{2} \cdot U^2 h} = 2.0 \end{cases}$$

(iii) Parameters of wave equation

The amplitude of the end of the body is set to be one-seventh of the total length, which is three times of the amplitude of half of the body when the maximum of undulation is reached.

Table 1. Data for the simulation case (Units: mm)

section node	a	b_u	b_l	C_d
0	0	0	0	(section)
1	94.4	85.7	79.3	1.2
2	146.0	134.5	123.0	1.2
3	173.2	175.9	154.4	1.2
4	182.9	214.4	179.9	1.2
5	182.9	230.8	194.9	1.2
6	181.7	238.0	202.6	1.2
7	175.3	239.6	209.0	1.2
8	164.0	236.4	215.5	1.2
9	149.5	226.7	215.5	1.2
10	130.2	209.0	202.6	1.2
11	110.9	178.5	175.3	1.2
12	88.4	141.5	138.3	1.2
13	74.0	107.7	96.5	1.2

14	54.7	146.2 (70.7)	111.2 (65.9)	2.0
15	0	209.4	174.3	2.0
16	0	255.5	222.9	2.0
17	0	299.3	247.1	2.0
18	0	309.0	242.3	2.0

c_1 and c_2 of the second-order amplitude envelope that bounds the wave equation were chosen to be -0.02 and 0.12,.

For body wave number k and frequency μ, we can set their values by giving body wavelength a and period T_{body} as:

$a = 3.2$ m , $k = \frac{2\pi}{a}$

$T_{body} = 4$ sec , $\mu = \frac{2\pi}{T_{body}}$

And the period of the exponential term which represents the initial delay when the body starts to undulate is given by the same value of the body wave period:

$T = T_{body}$

(iv) Results

First, let us see the case if the spring ratios for the motion of sway and yawing are both zero (i.e. without artificial springs). The program is calculated for 30 cycles and 10 time steps per cycle. We can see that there is a trend of drifting in the y direction and over-rotating of the angle ψ, and if the calculation is continued for as much as 40 total cycles, the motion of the body will be unstable or not calculable. (Figure 3,4)

Figure 5 to Figure 8 show the results after the artificial springs are added ($spring\ ratio_{sway}$=1 , $spring\ ratio_{yaw}$=1), the number of total calculated cycles are 40 and 10 time steps per cycle.

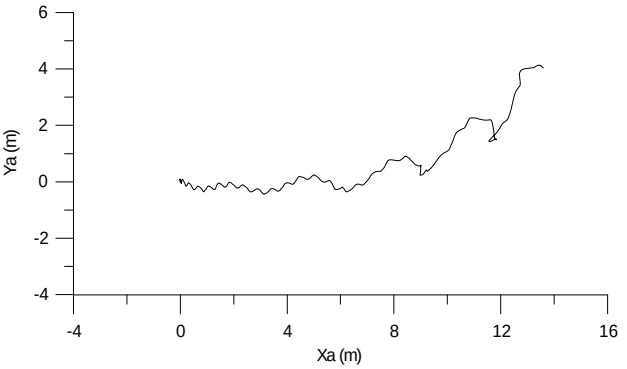

Figure 3 The trajectory of the body without artificial springs

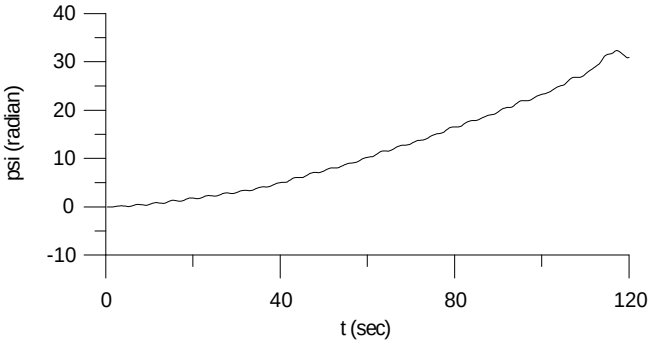

Figure 4 The angle ψ without artificial springs

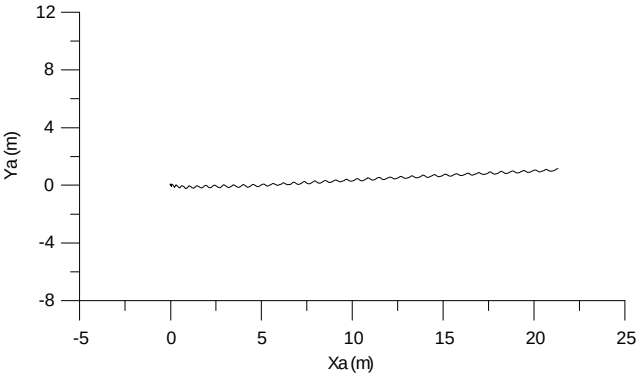

Figure 5 The trajectory of the body with artificial springs

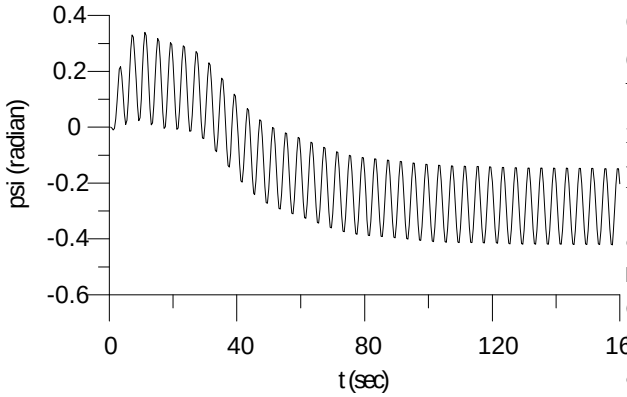

Figure 6 The angle ψ with artificial springs

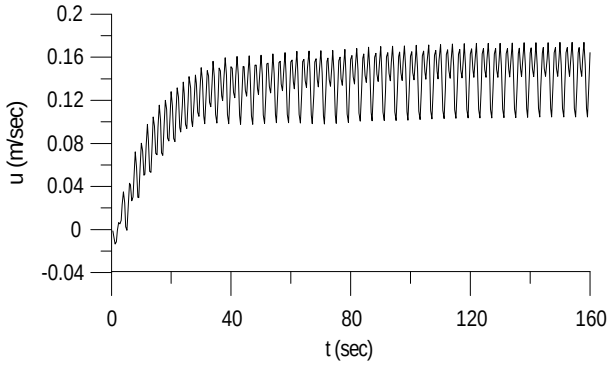

Figure 7 The velocity u with artificial springs

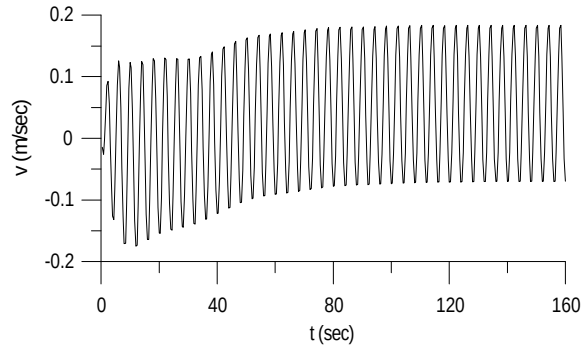

Figure 8 The velocity v with artificial springs

V. Conclusion

To study the motion of the fish-like underwater vehicle on the undulatory locomotion of a flexible slender body, this paper performs a simulation study based on the assumption of the potential theory. It is confirmed that reasonable results can be obtained. However, the results of the present simulation seem to be unstable without the added artificial springs in the motion of sway and yawing. By observations of real motion of fishes, the unstable condition may occur due to there are no side fins to balance the body. Thus, a better solution may be obtained in the future research by adding the effects of paired fins.

Furthermore, our theory is based on the assumption of the potential theory. The real motion of a fish-like body in fluid is more complicated with vortexes produced by the undulation of the body, and these vortexes may also be used in the propulsion. In the future development, it is necessary to have further consideration on the influence of vortexes to improve the validity of this simulation.

VI. References

[1] Lighthill, M. J., Mathematical Biofluiddynamics, Philadelphia: SIAM, 1975.

[2] Lighthill, M. J., "Note on the swimming of slender fish", J. Fluid Mech., (1960), vol. 9, pp.305-317.

[3] Wu, T. Y., "Hydromechanics of swimming propulsion. Part 3. Swimming and optimum movements of slender fish with side fins", J. Fluid Mech., (1971), vol. 46, part 3, pp.545-568.

[4] Blake, R. W., Fish Biomechanics (ed. P. W. Webb & D. Weihs), 1983.

[5] Blake, R. W., Fish Locomotion, Cambridge University Press, 1983.

[6] Ostrowski, J. & Burdick, J., "The geometric mechanics of undulatory robotic locomotion", International Journal of Robotics Research 17, 7, (1998), pp.683-701.

[7] Ostrowski, J. & Burdick, J., "Gait kinematics for a serpentine robot", Proceedings – IEEE International Conference on Robotics and Automation 2, (1996), pp.1294-1299.

[8] Cheng, J. Y., Zhuang, L. X. & Tong, B. G., "Analysis of swimming three-dimensional waving plates", J. Fluid Mech., (1991), vol. 232, pp.341-355.

[9] Azuma, A., The Biokinetics of Flying and Swimming, 1992.

[10] Viedler, J. J. & Hess, F., "Fast continuous swimming of two pelagic predators, Saithe and Mackel: a kinematic analysis", Journal of Experimental

Biology 109, pp.209-228.
[11]Dewar,H.,“Studies of tropical tuna swimming performance: thermoregulation, swimming mechanics and energetics”, Ph’d. Thesis in Marine Biology University of California, San Diego (1993).
[12]Barrett, D., Grosenbaugh, M. & Triantafyllou, M., “The optimal control of a flexible hull robotic undersea vehicle propelled by an oscillating foil”, Proceedings of the IEEE Symposium on Autonomous Underwater Vehicle Technology, (1996), pp.1-9.